



## Nonlinear optical transmission and optical power limiting characteristics of axial bonding type tin(IV) porphyrins with different peripheral substituents at the meso-positions

M V Vijisha<sup>1</sup>, Reshma Joseph<sup>2</sup>, Sebastian Nybin Remello<sup>2</sup> and K Chandrasekharan<sup>1</sup>

<sup>1</sup>Laser and Nonlinear Optics Laboratory, Department of Physics,  
National Institute of Technology Calicut, Kozhikode- 673 601, India

<sup>2</sup>Department of Applied Chemistry, Cochin University of Science and Technology, Kochi- 682 022, India

Dedicated to Professor GVLN Rao

Nonlinear optical properties of a number of dihydroxy tin(IV) porphyrins with different functional groups at the periphery have been investigated by means of single beam Z-scan technique employed with a Q-switched Nd: YAG laser delivering 7 ns pulses at 532 nm at a repetition rate of 10 Hz. Open aperture Z-scan studies show that reverse saturable absorption (RSA) is the mechanism behind the nonlinear optical absorption in all samples and excited state absorption is the major contributing factor to RSA. Nonlinear absorption coefficient was found to be higher for the tin(IV) porphyrin having carboxylate group (abbreviated as SnTCP) at the meso-positions. Optical limiting threshold value for SnTCP was estimated as  $\sim 0.67 \text{ J/cm}^2$ , which indicates its potentiality as an optical limiter for the smart filtering of optical energy in direct viewing systems. Closed aperture Z-scan results show that all the samples other than SnTPP exhibit self-defocusing nonlinearity and the magnitude of nonlinear refractive index is found to be nearly the same for all compounds. No closed aperture Z-scan signal was obtained for SnTPP, indicating that the dispersive contribution to the optical nonlinearity, in this case, is too small to be detected. © Anita Publications. All rights reserved.

doi.10.54955/AJP.30.12.2021.1673-1681

**Keywords:** Nonlinear optical properties, Z-scan, Porphyrin, Reverse saturable absorption, self defocusing.

### 1 Introduction

$\pi$ -conjugated organic molecules have been identified as excellent candidates for use in applications such as photodynamic therapy, optical data storage, optical limiting, information processing etc. not only because of their large and fast nonlinear optical response, but also due to the flexibility they offer in structural modifications [1-4]. Porphyrins are well renowned among the nonlinear optical organic molecules studied so far, owing to their two-dimensional structure and unique electronic properties [5]. The highly conjugated 18- $\pi$  electron system present in the porphyrin macrocycle which consists of four pyrrole units connected through four methine bridges is responsible for the NLO properties of porphyrin systems [6]. By core metalation and/or through peripheral functionalization, NLO response of these molecules can be drastically varied [7,8]. Incorporation of metal ions into the porphyrin cavity results in the extension of the  $\pi$ -electron delocalization and this leads to enhanced NLO activity in metalloporphyrins [9]. Tin(IV) porphyrins are advantageous in many ways over other metal-centered porphyrins. They are found to be very stable and are easy to synthesize [10,11]. Due to the presence of highly charged Sn(IV) ion, tin(IV) porphyrins are considered as the most readily ring reduced compounds among the metalloporphyrins studied so far [12].

Corresponding author

e mail: [csk@nitc.ac.in](mailto:csk@nitc.ac.in) (K Chandrasekharan);

Moreover, they exhibit favourable photophysical properties towards nonlinear optical applications. Here, we investigate the nonlinear optical transmission properties of a series of di-hydroxy tin(IV) porphyrins with different functional groups at the periphery (when phenyl groups are attached at the four peripheral positions, it is abbreviated as SnTPP, for mesityl group - SnTMP, pyridyl group - SnTPyP and for carboxylate group - SnTCP). The molecular structures of the compounds are shown in Fig 1.

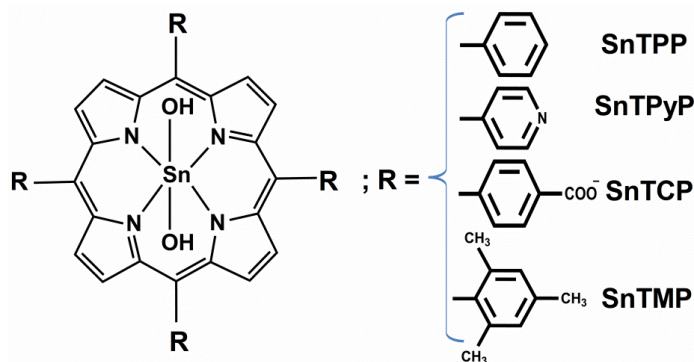


Fig 1. Molecular structures of tin(IV) porphyrins under study.

## 2 Experimental

The tin(IV) porphyrin samples were synthesized using a protocol reported elsewhere [11,14] and column chromatography was performed for the purification of the synthesized samples. For Z-scan measurement, appropriate amount of the sample was dissolved in spectroscopic grade diacetone alcohol under ultrasonication for 1 hour and was diluted to have a linear transmittance of about 65% at 532 nm.

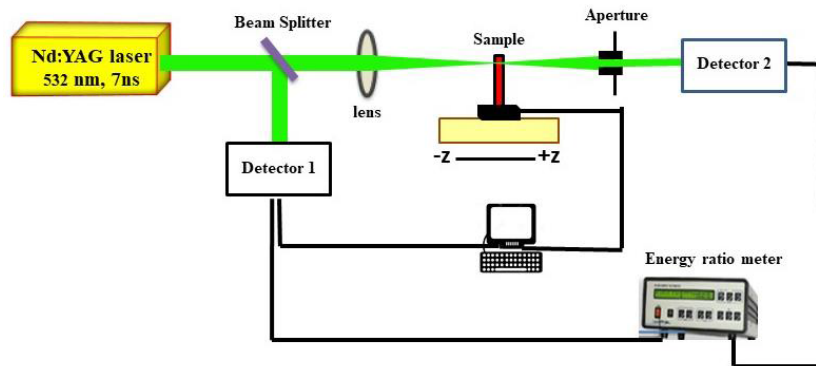


Fig 2. Schematic of Z-scan experimental set

The absorbance spectra of the porphyrin samples were measured using a UV/Vis Spectrophotometer (UV-2450 Shimadzu) and, a luminescence spectrometer (Perkin Elmer LS 55) was used to record the steady state fluorescence spectra of the samples. NLO characterization of the samples were done by means of Z-scan technique [15,16]. We used a Q-switched Nd: YAG laser (Quanta-Ray INDI-40) as the excitation source in Z-scan experiments (Fig 2). The laser source delivers pulses at 532 nm with pulse width of 7 ns at a repetition rate of 10Hz. The laser light beam was then split into two using a beam splitter. One beam was considered as the reference beam and the second beam was allowed to be incident on the sample. A convex lens having a focal length of 15 cm was used for this purpose. To find the laser beam spot size, knife edge (diamond edge) method was used. The spot size value came out to be  $\sim 17 \mu\text{m}$  and thus the Rayleigh range was found to be  $\sim 1.7 \text{ mm}$ . A 1 mm thick quartz cuvette was used as the sample cell

so that thin sample approximation condition can be made valid. The sample cell was then placed on a computer driven translational stage to move the sample along the axis of the focused beam. The incident as well as transmitted energies were detected and recorded using two pyroelectric detectors (RjP-735, Laser Probe. Corp., USA) and an energy ratio meter (Rj-7620, Laser Probe Corp., USA). To study the nonlinear absorptive as well as refractive properties of samples, Z-scan was operated in both open aperture (OA) and closed aperture (CA) configurations, respectively. CA Z-scan studies were accomplished by placing an aperture having a diameter of 3 mm in front of the detector placed in the path of transmitted beam.

### 3 Result and Discussion

The optical absorption and emission spectra of SnTPP, SnTPyP, SnTMP and SnTCP, dissolved in diacetone alcohol are shown in Fig 3.

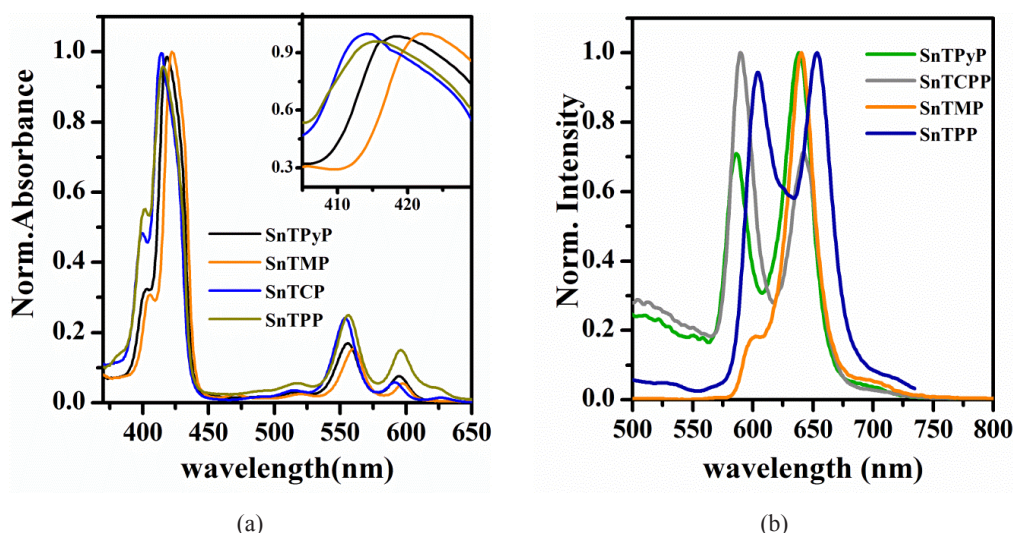


Fig 3. (a) Absorption (magnified view of the Soret peaks is given in the inset) and (b) emission spectra of SnTMP, SnTCP, SnTPP and SnTPyP.

All the tin (IV) porphyrin samples show an intense Soret band with a shoulder peak, in blue wavelength region corresponding to the strongly allowed  $S_0 \rightarrow S_2$  transition, and two relatively weak Q bands which are due to the  $S_0 \rightarrow S_1$  transition [11]. The Soret peaks are situated in the spectral region 410-425 nm while Q band peaks are located within 550-600 nm. All samples exhibit very small, but definite absorption at 532nm, wavelength used for nonlinear optical studies. It can be seen from Fig 3(a) that the shift in the position of Q-bands towards the longer wavelength region is according to the increasing order of electron donating character of the peripheral groups. Steady state fluorescence spectra (Fig 3(b)) of all compounds except SnTMP, show two strong distinct emission peaks within 580-600 nm and 635-660 nm corresponding to  $S_1 \rightarrow S_0$  transition, upon excitation near the Soret band. Both the absorption and emission band positions are related to the size of the delocalized  $\pi$ -system [17]. In general, electronic spectra of tin porphyrins show  $Q^*(0,0)$  and  $Q^*(0,1)$  emission bands (typical of porphyrins) with either mirror image relationship or reverse mirror image relationship. In our case, we observed a mirror image relationship with  $Q^*(0,0) : Q^*(0,1)$  ratio less than 1. Also, it should be noted that the emission intensity of  $Q^*(0,1)$  for SnTMP is much higher than that of the  $Q^*(0,0)$  band (the  $Q^*(0,0)$  peak is very weak). These intensity variations of the emission peaks can be attributed to the steric effect of the meso aryl substitution. Generally metal porphyrins with bulkier groups at the meso positions will have the most planar porphyrin ring and, in the case of SnTMP with mesityl meso substitution, the two ortho methyl groups can sterically hinder the rotation about the meso C-C bond making

the SnTMP system more planar. This causes a decrease in the resonance interactions between the porphyrin core and the meso substituent which in turn leads to a reduction in the fluorescence yield of the compound [18H2T(2-Cl,19)]. Also, the presence of bulkier groups will decrease the rate of radiative decay and, increase the rate of non-radiative process by promoting intersystem crossing. This further diminishes the intensity of  $Q^*(0,0)$  emission of SnTMP.

Open aperture Z-scan measurements were carried out for the porphyrin compounds at an intensity of  $0.27 \text{ GW/cm}^2$  and the obtained OA Z-scan curves are shown in Fig 4. Closer to the beam focus where the laser fluence is high, the transmittance through the samples is found to be deviated from Beer's law and shows an intensity dependent behaviour. This indicates that all the samples exhibit significant nonlinear absorption when excited with 7ns laser pulses. We also performed Z-scan experiment at different input energies, to check the nonlinear response of diacetone alcohol solvent. For all input energies, the solvent did not show any Z-scan signal and thus, the observed nonlinearity of the porphyrin solution samples can be considered as due to the porphyrin molecules only.

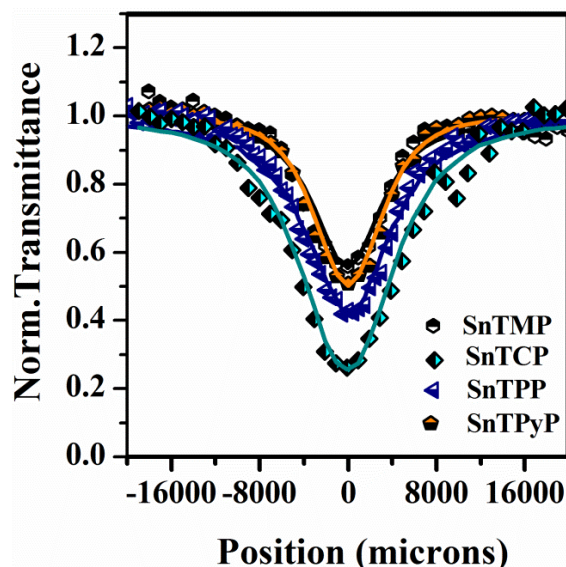


Fig 4. The OA Z-scan traces of SnTMP, SnTCP, SnTPP and SnTPyP at an intensity of  $0.27 \text{ GW/cm}^2$ .

The principal mechanisms behind NLA in materials include saturable absorption (SA) and/or reverse saturable absorption (RSA). The OA Z-scan signatures of the samples suggest that all the porphyrin compounds under study exhibit RSA behaviour. As can be seen from Fig 4, the transmission drop is greater for SnTCP, indicating that strength of RSA effects is higher in this case. In general, RSA in material media can be caused by two phenomena- two-photon absorption (TPA) and excited state absorption (ESA). The mechanism responsible for RSA can be figured out by determining the nonlinear absorption coefficient ( $\beta_{eff}$ ) for each porphyrin sample, which can be done by making best fit of OA Z-scan data using appropriate nonlinear optical propagation equations [20,21]. Best fit to the measured data was obtained for SA assisted effective TPA model for which nonlinear propagation equation is given by

$$\frac{dI}{dz} = - \left[ \frac{\alpha_0}{1 + (II_s)} + \beta_{eff} I \right] I \quad (1)$$

where  $z$ , represents the propagation length of the laser beam inside the sample,  $\alpha_0$  is the linear absorption coefficient and,  $I$  and  $I_s$  stand for input laser intensity and saturation intensity, respectively. Nonlinear optical

absorption coefficient,  $\beta_{eff}$  was determined by numerically fitting the OA Z-scan data to nonlinear propagation equation ( Eq (1)). The term ‘effective TPA’ is used in connection with the fact that both genuine TPA and ESA can have significant contributions to the absorptive nonlinearity. Since it is challenging to distinguish the contributions of these two effects via the NLO transmittance measurement in the nanosecond-picosecond range, the term “effective nonlinear absorption coefficient ( $\beta_{eff}$ )” is used to label the NLA on the microscopic level under these excitation conditions [1,2]. Saturation of absorption (SA) plays a role here, even though it is not visible. However, as expected, we observed  $I_s$  to be very high.

The solid lines in Fig 4 represent the fits to the measured data, obtained using Eq (1) in which  $\beta_{eff}$  and  $I_s$  were used as the fitting parameters. The magnitude of  $\beta_{eff}$  was found to be in the order SnTCP > SnTPP > SnTPyP > SnTMP and the values are tabulated in Table 1.

Table 1. Measured nonlinear optical parameters of tin (IV) porphyrin samples and comparison with a few reported works

	$\beta_{eff}$ (cm/GW)	$\Delta\Phi$	$n_2$ ( $10^{-17}\text{m}^2/\text{W}$ )	Limiting Threshold ( $\text{J}/\text{cm}^2$ )
SnTPP	136	---	---	1.35
SnTPyP	103	-1.22	-4.6647	1.81
SnTMP	79	-1.22	-4.67157	---
SnTCP	240	-1.04	-2.12014	0.67
Sn(IV)MHTP(OH) <sub>2</sub> , Krishna <i>et al</i> [22]	168	---	---	---
SnTTP, Kiran <i>et al</i> [23]	---	---	---	12.30
Graphene-TPP, Liu <i>et al</i> [24]	142	---	---	---

where  $n_2$  is nonlinear refraction coefficient

In our case, the porphyrin compounds under study, have definite absorption at the laser excitation wavelength suggesting that the major contribution to the observed NLA behaviour of the samples can be from ESA rather than TPA. Also, with nanosecond laser pulses, the occurrence of ESA is more probable than TPA [25]. However, we cannot completely ruled out the NLA contribution from TPA, since all the studied porphyrin compounds have definite absorption in the off-resonant lower wavelength region also. To understand the exact phenomena involved in NLA, we performed Z-scan of the porphyrin compounds at different input beam energies. Figure 4 shows the dependence of  $\beta_{eff}$  on the on-axis input irradiance. From figure, it can be seen that the maximum NLA occurs at an input intensity of  $0.27\text{GW}/\text{cm}^2$  and at higher intensities, the value of  $\beta_{eff}$  falls down showing that the contribution to RSA is mainly from ESA. This is due to the fact that if ESA is the prominent mechanism behind NLA, then exciting the material media with high intense optical radiation can cause considerable depletion in the ground state population due to greater ESA cross sections. This eventually leads to the intensity dependence of  $\beta_{eff}$  [21].

The incorporation of tin(IV) at the porphyrin cavity results strong spin-orbit interaction among the orbitals of tin(IV), and it also causes the mixing of metal orbitals with that of the porphyrin ring. This spin-orbit interaction influences the intersystem crossing (ISC) rate in such a way that ISC rate increases with the spin-orbit coupling strength. Higher ISC rate increases the chance for ESA and thus RSA [26,27]. To elucidate the elevated NLA response of SnTCP, several factors have to be taken into account. SnTCP is anionic in nature. The -COOH substituent is in the deprotonated state under neutral condition (possible counter ion is Cl-) and hence it can undergo H-aggregation by  $\pi$  stacking. There is also a possibility of J-aggregation in which two porphyrin rings are stacked by diagonally opposite carboxyl of third porphyrin ring by interaction through Sn. Another contributing factor can be the electron withdrawing nature of the meso -COO- substitution. In fact, it is the only meso substitution with a negative Hammett constant. Moreover, in all the studied porphyrin

samples, except in the case of SnTMP, the porphyrin ring is in resonance with the meso substitution and hence  $\pi$ -electron delocalization is possible. In SnTCP, the dihedral angle becomes smaller due to the carboxyl substituent and thus, one can expect more  $\pi$ -electron delocalization in SnTCP [18].

Optical power limiting (OPL) refers to the property of a material to reduce light transmission at higher input fluences [28]. Materials exhibiting NLO behaviour such as nonlinear absorption, nonlinear refraction, nonlinear scattering etc. can possess OPL property [29,30] and are thus called optical limiters. The applications of optical limiters include the protection of sensitive optical devices and human eye from high intense light, all-optical switching etc. [31-33]. For studying the OPL performance of the samples, nonlinear transmittance data were extracted from the corresponding OA Z-scan traces and plotted against input fluence. The OPL (optical power limiting) curves of tin(IV) porphyrins are shown in Fig 6. In the porphyrin samples under consideration, RSA process is responsible for the OPL action. The limiting threshold, defined as the fluence at which the transmittance falls to 50% of its normalized value, is noted in each case and is found to be minimum for SnTCP, which is  $0.67 \text{ J/cm}^2$ . Poor OPL action is observed for SnTMP at  $0.27 \text{ GW/cm}^2$ , which can be attributed to its relatively weaker RSA effects.

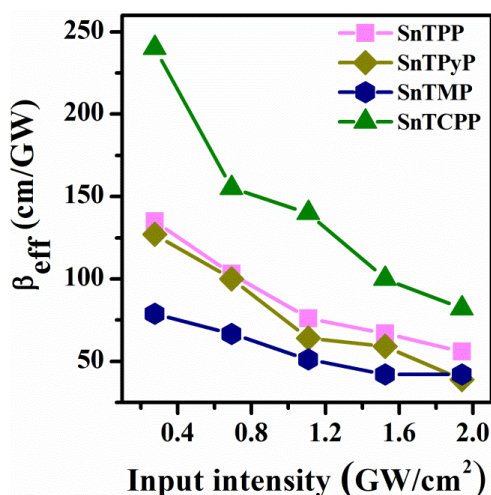


Fig 5.  $\beta_{eff}$  v/s on-axis input irradiance plot for tin(IV) porphyrin samples

To examine the nonlinear refraction (NLR) properties of the tin(IV) compounds, CA Z-scan measurements were done. In general, CA Z-scan data comprises of both nonlinear absorption as well as refraction properties of samples. To extract the NLR properties alone, closed by open (CBO) method in which the CA Z-scan data was divided by the corresponding OA Z-scan data, was used. Figure 6 shows the CBO curves obtained at an input intensity of  $0.27 \text{ GW/cm}^2$ . The solid line curves shown in the figure represent the numerical fits to the measured data and the fit was obtained using equation given by [34],

$$T(z) = 1 + \frac{4\Delta\phi_0(z/z_0)}{[1 + (z/z_0)^2][9 + (z/z_0)^2]} \quad (2)$$

Here  $\Delta\phi_0$  stands for the on-axis nonlinear phase shift at the focal point. As can be inferred from the NLR profiles shown in Fig 6, all the porphyrin samples disclose the presence of negative NLR which can be understood as the result of self-defocusing effect. Negative NLR points out to the occurrence of thermal lensing effect and is an expected phenomenon when excited with nanosecond laser pulses [35]. The variation in refractive index due to thermal lensing can be expressed as  $\Delta n = (\partial n / \partial T) \Delta T$ , where  $\partial n / \partial T$  represents the refractive index change of the material medium with respect to temperature and  $\Delta T$  is the temperature change due to the laser beam [9,36]. We also conducted CA Z-scan analysis of the samples at higher input intensities

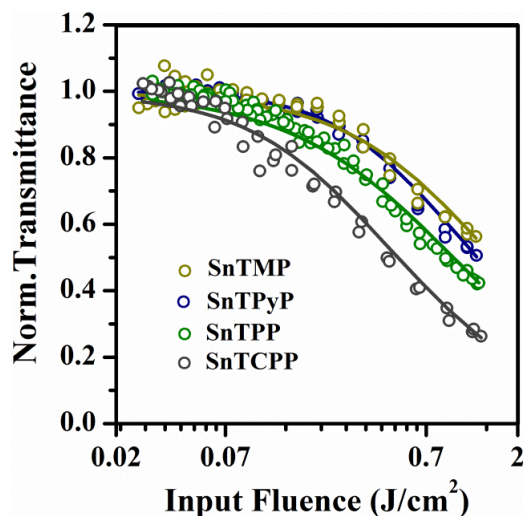


Fig 6. Optical limiting curves of tin(IV) porphyrin samples at  $0.27\text{GW}/\text{cm}^2$ . Solid lines are the numerical fits.

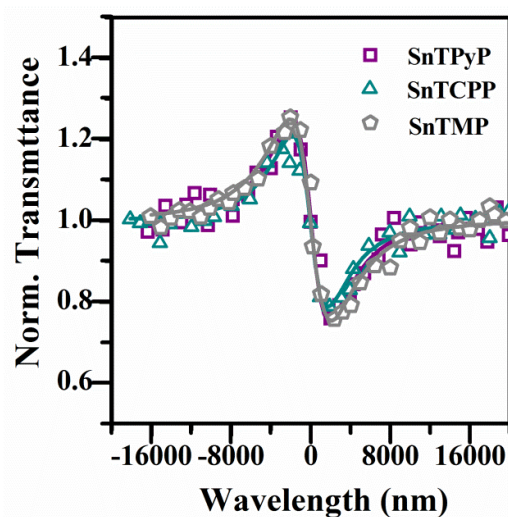


Fig 7. The CBO curves of tin(IV) porphyrins at  $0.027\text{GW}/\text{cm}^2$ .

and we did not observe any significant changes in the CA Z-scan signature. The self defocusing nature of the samples remained unaltered at higher intensities. The nonlinear refraction coefficient  $n_2$  can be computed using the equation,

$$n_2(m^2/w) = \frac{\lambda \Delta\phi_0}{2\pi I_0 L_{eff}} \quad (3)$$

The values obtained for the nonlinear refraction coefficients are tabulated in Table 1 and can be considered as the consequence of the synergetic effect between the thermal and electronic contributions to the refractive nonlinearity. It was observed that SnTPP did not show any CA Z-scan signal implying that the dispersive contribution to its optical nonlinearity is negligibly small. All compounds other than SnTPP showed nearly the same values for the nonlinear refraction coefficient,  $n_2$ . This may be due to the fact that the influence of the electronic nature of peripheral groups on the direction of dipole moment is relatively small.

#### 4 Summary

In summary, we have investigated the NLO properties of a set of tin(IV) porphyrins with peripheral modifications, using Z-scan technique under nanosecond regime. All the porphyrin compounds under study were found to exhibit profound NLA and the responsible mechanism behind NLA was recognized as ESA assisted RSA. The NLA behaviour of SnTCP was found to be highest among the studied compounds and the possible reasons for its elevated optical nonlinearity include aggregate formation and the increased  $\pi$ -electron delocalization resulting from the lesser dihedral angle due to the carboxyl group substitution. SnTCP also revealed higher optical limiting efficiency with an optical limiting threshold value of  $\sim 0.67 \text{ J/cm}^2$ . Considering the refractive optical nonlinearity, self defocusing effect was observed in all samples, except in SnTPP and the  $n_2$  values were found to be nearly the same in these compounds.

#### References

1. Du Y, Dong N, Zhang M, Zhu K, Na R, Zhang S, Sun N, Wang G, Wang J, Covalent Functionalization of Graphene Oxide with Porphyrin and Porphyrin Incorporated Polymers for Optical Limiting, *Phys Chem Chem Phys*, 19(2017) 2252–2260.
2. Makhal K, Arora S, Kaur P, Goswami D, Singh K Third-order nonlinear optical response and ultrafast dynamics of tetraoxa [22] porphyrin(2.1.2.1)s, *J Mater Chem C*, 4(2016)9445–9453.
3. Singh K, Arora S, Makhal K, Kaur P, Goswami D, Nonlinear absorption in tetrathia [22] porphyrin(2.1.2.1)s: Visualizing strong reverse saturable absorption at non-resonant excitation, *RSC Adv*, 6(2016)22659–22663.
4. Rao S V, Srinivas NKMN, Rao D N, Giribabu L, Maiya B G, Philip R, Kumar G R, Studies of third-order optical nonlinearity and nonlinear absorption in tetra tolyl porphyrins using degenerate four wave mixing and Z-scan, *Opt Commun*, 182(2000)255–264.
5. Jiang L, Lu F, Li H, Chang Q, Li Y, Liu H, Wang S, Third-Order Nonlinear Optical Properties of an Ultrathin Film Containing a Porphyrin Derivative, *J Phys Chem B*, 109(2005)6311–6315.
6. Calvete M, Ying G, Hanack M, Porphyrins and phthalocyanines as materials for optical limiting, *Synth Met*, 141(2004)231–243.
7. Vijisha M V, Ramesh J, Arunkumar C, Chandrasekharan K, Nonlinear optical absorption and refraction properties of fluorinated trans-dicationic pyridinium porphyrin and its metal complexes, *Opt Mater*, 98(2019)109474; doi.org/10.1016/j.optmat.2019.109474.
8. Senge M O, Fazekas M, Notaras EGA, Blau W J, Zawadzka M, Locos O B, Mhuircheartaigh EMN, Nonlinear optical properties of porphyrins, *Adv Mater*, 19(2007)2737–2774.
9. Narendran N K S, Soman R, Sankar P, Arunkumar C, Chandrasekharan K, Ultrafast and short pulse optical nonlinearities of meso-tetrakis-(2,3,5,6-tetrafluoro-N,N,N-trimethyl-4-aniliniumyl) porphyrin and its metal complexes, *Opt Mater*, 49(2015)59–66.
10. Sayer P, Gouterman M, Connell C, Metalloid porphyrins and phthalocyanines, *Acc Chem Res*, 15(1982)73–79.
11. Soman R, Raghav D, Sujatha S, Rathinasamy K, Arunkumar C, Axial ligand modified high valent tin(IV) porphyrins: synthesis, structure, photophysical studies and photodynamic antimicrobial activities on *Candida albicans*, *RSC Adv*, 5(2015)61103–61117.
12. Arnold D P, Blok J, The coordination chemistry of tin porphyrin complexes, *Coord Chem Rev*, 248(2004)299–319.
13. Thomas A A, Kuttassery F, Protolytic behavior of axially coordinated hydroxy groups of Tin (IV) porphyrins as promising molecular catalysts for water oxidation, *J Photochem Photobiol A: Chem*, 358(2018)402–410.
14. Thomas A, Kuttassery F, Remello S N, Mathew S, Yamamoto D, Onuki S, Nabetani Y, Tachibana H, Inoue H, Facile synthesis of water-soluble cationic tin (IV) porphyrins and water-insoluble tin(IV) porphyrins in water at ambient temperature, *Bull Chem Soc Jpn*, 89(2016)902–904.
15. Sheik-bahae M, Said A A, Van Stryland E W, High-sensitivity, single-beam  $n_2$  measurements, *Opt Lett*, 14(1989) 955–957.
16. Sheik-Bahae M, Said A A, Wei T-H, Hagan D J, Van Stryland E W, Sensitive measurement of optical nonlinearities using a single beam, *IEEE J Quant Electron*, 26(1990)760–769.

17. Kulyk B, Taboukhat S, Akdas-Kilig H, Fillaut J-L, Boughaleb Y, Sahraoui B, Nonlinear refraction and absorption activity of dimethylaminostyryl substituted BODIPY dyes, *RSC Adv*, 6(2016)84854–84859.
18. Zakavi S, Hoseini S, The absorption and fluorescence emission spectra of meso-tetra(aryl)porphyrin dications with weak and strong carboxylic acids: A comparative study, *RSC Adv*, 5(2015)106774–106786.
19. Fonda H N, Gilbert J V, Cormier R A, Sprague J R, Kamioka K, Connolly J S, Spectroscopic, photophysical, and redox properties of some meso-substituted free-base porphyrins, *J Phys Chem*, 97(1993)7024–7033.
20. Van Stryland E W, Wu Y Y, Hagan D J, Soileau M J, Mansour K, Optical limiting with semiconductors, *J Opt Soc Am B*, 5(1988)1980–1988.
21. Vijisha M V, Sini V V, Narendran N K S, Chandrasekharan K, Enhanced nonlinear optical response from dihydroxy(5,10,15,20-tetraphenyl porphyrinato)tin(IV) or SnTPP in a fully plastic photonic crystal microcavity, *Phys Chem Chem Phys*, 19(2017)29641–29646.
22. Krishna M B M, Venkatramaiah N, Venkatesan R, Rao D N, Synthesis and structural, spectroscopic and nonlinear optical measurements of graphene oxide and its composites with metal and metal free porphyrins, *J Mater Chem*, 22(2012)3059–3068.
23. Kiran P P, Reddy D R, Maiya B G, Dharmadhikari A K, Kumar G R, Rao D N, Nonlinear absorption properties of “axial-bonding” type tin(IV) tetratolylporphyrin based hybrid porphyrin arrays, *Opt Commun*, 252(2005)150–161.
24. Liu Z, Xu Y, Zhang X, Zhang X, Chen Y, Tian J, Porphyrin and Fullerene Covalently Functionalized Graphene Hybrid Materials with Large Nonlinear Optical Properties, *J Phys Chem B*, 113(2009)9681–9686.
25. Sreekanth P, Sridharan K, A. Rose Abraham, H.P. Janardhanan, N. Kalarikkal, R. Philip, Nonlinear transmittance and optical power limiting in Magnesium ferrite nanoparticles: effects of laser pulsewidth and particle size, *RSC Adv*, 6(2016)106754–106761.
26. B. Aneeshkumar, P. Gopinath, J. Thomas, C.P.G. Vallabhan, V.P.N. Nampoori, P. Radhakrishnan, Nanosecond optical limiting response of sandwich-type neodymium diphthalocyanine in a co-polymer host, 143(2004)197–201.
27. Singh B P, Effects of Metal Substitution on Third-order Optical Non-linearity of Porphyrin Macrocycle, *J Porphyr Phthalocyanines*, 86(1999)81–86.
28. Girisun T C S, Saravanan M, Rao S V, Enhanced broadband optical limiting and switching of nonlinear absorption in functionalized solar exfoliated reduced graphene oxide-Ag-Fe<sub>2</sub>O<sub>3</sub> nanocomposites, *J Appl Phys*, 124(2018)193101; doi.org/10.1063/1.5050478.
29. Tutt L E E W, Boggess T F, Company E K, A review of optical limiting mechanisms and devices using organics, fullerenes, semiconductors and other materials, *Prog Quantr Elecrr*, 17(1993)299–338.
30. Spangler C W, Recent development in the design of organic materials for optical power limiting, *J Mater Chem*, 9(2013)2013–2020.
31. Polavarapu L, Ji W, Xu Q, Optical-Limiting Properties of Oleylamine-Capped Gold Nanoparticles for Pulses, *ACS Appl Mater Interfaces*, 1(2009)2298–2303.
32. Dini D, Calvete M J F, Hanack M, Nonlinear Optical Materials for the Smart Filtering of Optical Radiation, *Chem Rev*, 116(2016)13043–13233.
33. Lindsey J S, Wagner R W, Investigation of the synthesis of ortho-substituted tetraphenylporphyrins, *J Org Chem*, 54(1989)828–836.
34. Kulyk B, Taboukhat S, Akdas-Kilig H, Fillaut J L, Boughaleb Y, Sahraoui B, Nonlinear refraction and absorption activity of dimethylaminostyryl substituted BODIPY dyes, *RSC Adv*, 6(2016)84854–84859.
35. Jiang L, Jiu T, Li Y, Li Y, Yang J, Li J, Li C, Excited-State Absorption and Sign Tuning of Nonlinear Refraction in Porphyrin Derivatives, *J Phys Chem B*, 112(2008)756–759.
36. Kovsh D I, Hagan D J, Van Stryland E W, Numerical modeling of thermal refraction in liquids in the transient regime, *Opt Express*, 4(1999)315–327.

[Received: 02.08.2021; revised recd: 16.09.2021; accepted: 03.10.2021]